How to cite: *Angew. Chem. Int. Ed.* **2024**, *63*, e202320214
doi.org/10.1002/anie.202320214

Polymer Chemistry | Hot Paper

Redesigned Nylon 6 Variants with Enhanced Recyclability, Ductility, and Transparency

Jun-Jie Tian, Xiaoyang Liu, Liwei Ye, Zhen Zhang, Ethan C. Quinn, Changxia Shi, Linda J. Broadbelt, Tobin J. Marks,* and Eugene Y.-X. Chen**

Abstract: Geminal (*gem*−) disubstitution in heterocyclic monomers is an effective strategy to enhance polymer chemical recyclability by lowering their ceiling temperatures. However, the effects of specific substitution patterns on the monomer's reactivity and the resulting polymer's properties are largely unexplored. Here we show that, by systematically installing *gem*-dimethyl groups onto ε-caprolactam (monomer of nylon 6) from the α to ε positions, both the redesigned lactam monomer's reactivity and the resulting *gem*-nylon 6's properties are highly sensitive to the substitution position, with the monomers ranging from non-polymerizable to polymerizable and the *gem*-nylon properties ranging from inferior to far superior to the parent nylon 6. Remarkably, the nylon 6 with the *gem*-dimethyls substituted at the γ position is amorphous and optically transparent, with a higher T_g (by 30 °C), yield stress (by 1.5 MPa), ductility (by 3×), and lower depolymerization temperature (by 60 °C) than conventional nylon 6.

Nylons (aliphatic polyamides or PAs) find extensive applications in diverse industries such as textiles, engineering plastics, automotive components, packaging, and fishing equipment, due to their high-performance characteristics.[1,2] However, nylon's robustness and environmental persistence come with a significant environmental concern due to their high resistance to conventional chemical recycling methods and biodegradation, leading to the growing accumulation of nylon-based plastics or fiber waste in landfills and natural environments.[3] For instance, discarded or lost nylon materials as fishing gear constitute a substantial portion of ocean plastic pollution, accounting for about 10 % of all ocean plastic and over 40 % of the Great Pacific Garbage Patch.[4] This pollution poses a continuous threat to the global marine ecosystems.[4a,5] As a result, there is an urgent need to recycle nylons and to establish a circular economy to address the growing challenges posed by nylon-based plastic pollution.

Nylon 6, the most prevalent PA in the nylon family, is manufactured industrially via ring-opening polymerization (ROP) of seven-membered ε-caprolactam (7LM)[6] and currently holds a dominant position in the nylon market, accounting for a significant portion of global revenue, with a market share exceeding 56.0 %.[2c] However, the recycling of post-consumer nylon 6 waste significantly lags behind its production volume.[7] Of the 4.4 million tonnes of annual global nylon 6 production, less than 2 % contains nylon 6 derived from the recycled monomer.[8] Chemical recycling to monomer (CRM) presents an attractive approach to nylon 6 recycling, enabling the recycled 7LM to be repolymerized to the same polymer.[9] Efforts have been devoted to developing more efficient catalysts and conditions to reduce the energy input into depolymerization of nylon 6 by using ionic liquids[10] and Ru-catalyzed hydrogenative deconstruction of nylons.[11] Very recently, Marks et al. demonstrated efficient CRM of nylon 6 to 7LM at 220–240 °C using highly reactive lanthanide/early-transition metal catalysts with high catalyst turnover frequencies and 7LM recovery yields.[12] Nevertheless, these approaches do not fully address the limitations in the intrinsic recyclability of nylon 6 due to the high ring strain and ceiling temperature (T_c) of 7LM.[13] Hence, there is a need to redesign nylon 6 via modification of 7LM, aiming to develop new nylon 6 derivatives with enhanced chemical recyclability (Scheme 1). Furthermore, structural modification of the nylon 6 backbone may impart unique properties such as enhanced ductility and optical clarity that the parent nylon 6 lacks, thereby expanding nylon 6's applications.

According to the design principles for intrinsically circular polymers,[14] to enhance chemical recyclability (rendering lower depolymerization temperature and higher selectivity for pure monomer recovery), it is essential to

[*] Dr. J.-J. Tian, Dr. Z. Zhang, E. C. Quinn, Dr. C. Shi, Prof. Dr. E. Y.-X. Chen
Department of Chemistry, Colorado State University
Fort Collins, CO 80523-1872 (USA)
E-mail: eugene.chen@colostate.edu
Dr. X. Liu, Prof. Dr. L. J. Broadbelt
Department of Chemical and Biological Engineering, Northwestern University
2145 Sheridan Road, Evanston, IL 60208-3113 (USA)
E-mail: broadbelt@northwestern.edu
Dr. L. Ye, Prof. Dr. T. J. Marks
Department of Chemistry and the Trienens Institute for Sustainability and Energy, Northwestern University
2145 Sheridan Road, Evanston, IL 60208-3113 (USA)
E-mail: t-marks@northwestern.edu

© 2024 The Authors. Angewandte Chemie International Edition published by Wiley-VCH GmbH. This is an open access article under the terms of the Creative Commons Attribution Non-Commercial License, which permits use, distribution and reproduction in any medium, provided the original work is properly cited and is not used for commercial purposes.

© 2024 The Authors. Angewandte Chemie International Edition published by Wiley-VCH GmbH

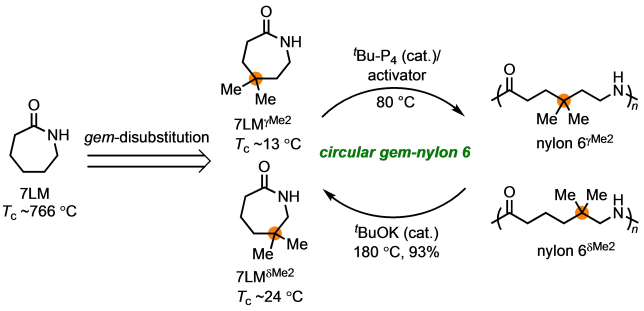

Scheme 1. Lactam monomer design for nylon 6 variants with enhanced chemical recyclability via *gem*-disubstitution. T_c values extrapolated to 1.0 M.

reduce the high T_c (~766 °C, see below) of 7LM. The geminal (*gem*−) disubstitution strategy has been validated as an effective approach to enable or enhance the chemical recyclability of polymers back to their heterocyclic monomers, attributable to the Thorpe–Ingold effect.[15,16] Recent reports disclosed that the introduction of *gem*-disubstitution into β-butyrolactone[17] and valerolactone[18] at the α position enables or significantly enhances chemical recyclability. However, the effects of *gem*-disubstitution patterns or positions in heterocyclic monomers on the monomer's reactivity and the polymer's recyclability and performance are largely unexplored. Here we utilize 7LM and its derivatives as an effective monomer platform in this study since it provides five possible positions (from α to ε positions, Scheme 2) for the systematic installation of *gem*-dimethyl groups, which enables elucidation of monomer structure/reactivity and product polymer structure/property relationships. Moreover, it produces technologically informative nylon 6 variants with possibly enhanced chemical recyclability and performance properties such as mechanical ductility and optical transparency—the two properties the parent nylon 6 lacks which would be desirable.

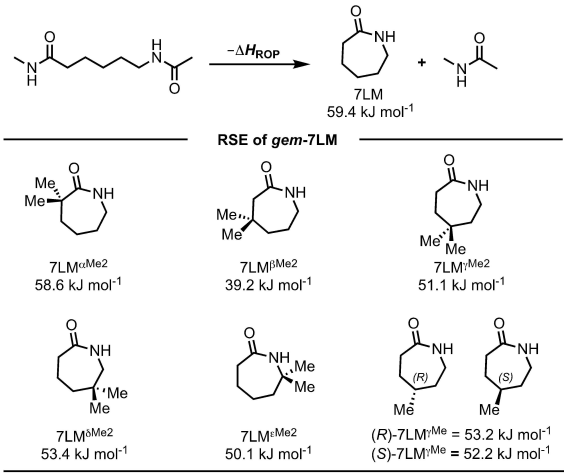

Scheme 2. Computed ring strain energies (RSEs) of 7LM-based monomers.

At the outset, we computed the ring strain energies (RSEs) of parent 7LM and *gem*-dimethylated 7LM monomers substituted at five different positions (α to ε), 7LM$^{\alpha Me2}$, 7LM$^{\beta Me2}$, 7LM$^{\gamma Me2}$, 7LM$^{\delta Me2}$, and 7LM$^{\varepsilon Me2}$, to determine if, and by how much, *gem*-disubstitution can reduce ring strain (Scheme 2). The estimation of RSEs was made by computing the ROP enthalpy of the lactams leading to linear polymers represented by one repeat unit, based on an isodesmic reaction. The *gem*-dimethyl group at the α position slightly influences the RSE, resulting in 7LM$^{\alpha Me2}$ with a high RSE of 58.6 kJ mol^{-1}, close to 7LM of 59.4 kJ mol^{-1}. When the *gem*-dimethyl group is moved to the β position, the RSE dramatically falls to 39.2 kJ mol^{-1} for 7LM$^{\beta Me2}$. Note that the RSEs of γ, δ, and ε-*gem*-7LMs (7LM$^{\gamma Me2}$, 7LM$^{\delta Me2}$, 7LM$^{\varepsilon Me2}$) are considerably lower than 7 ML by 6–9 kJ mol^{-1}. For comparative purposes, the RSEs of γ-monomethyl 7LM (7LM$^{\gamma Me}$) were also calculated to be 53.2 kJ mol^{-1} for (*R*)-7LM$^{\gamma Me}$ and 52.2 kJ mol^{-1} for (*S*)-7LM$^{\gamma Me}$. These RSE data show that the introduction of the *gem*-dimethyl group into 7LM at all positions successfully reduces the RSE, with the α position creating the smallest reduction and the β position the largest reduction (~20 kJ mol^{-1}).

Subsequently, we synthesized the entire series of six 7LM monomers (Scheme 2) and investigated their polymerization under typical anionic ROP conditions,[19,20] using phosphazene superbase ^{t}Bu-P$_4$ or NaH as a base, *N*-benzoyl-substituted *gem*-7LM as an activator, and *N,N*-dimethylacetamide (DMAc) as solvent when added (Table S1–S6). Surprisingly, 7LMs with *gem*-dimethyl substitution at α, β, and ε positions, 7LM$^{\alpha Me2}$, 7LM$^{\beta Me2}$, and 7LM$^{\varepsilon Me2}$, did not yield the corresponding *gem*-nylon 6 under various conditions employed in this study (Tables 1, S1, S2 and S5). In contrast, when the dimethyl groups are introduced at the γ and δ positions, γ-*gem*-dimethylated nylon 6 (nylon 6$^{\gamma Me2}$) and δ-*gem*-dimethylated nylon 6 (nylon 6$^{\delta Me2}$) were successfully synthesized (Tables S3 and S4). For example, the ROP of 7LM$^{\gamma Me2}$ in DMAc with ^{t}Bu-P$_4$ as the base and *N*-benzoyl-substituted 7LM$^{\gamma Me2}$ as an activator achieved 64 % conver-

Table 1: Selected results for polymerization of substituted 7LMs.[a]

Run	M	[M]/[B]/[A]	Time (h)	Conv.[b] (%)	M_n[c] (kDa)	$Đ$[c]
1	7LM$^{\alpha Me2}$	100/1/1	24	0	–	–
2	7LM$^{\beta Me2}$	100/1/1	24	0	–	–
3	7LM$^{\gamma Me2}$	100/1/1	6	70	20.4	1.31
4[d]	7LM$^{\gamma Me2}$	500/5/1	12	64	47.2	1.41
5	7LM$^{\delta Me2}$	100/1/1	6	71	17.9	1.12
6[d]	7LM$^{\delta Me2}$	500/5/1	12	70	68.1	1.12
7	7LM$^{\varepsilon Me2}$	100/1/1	24	0	–	–
8	7LM$^{\gamma Me}$	100/1/1	12	88	33.5	1.39
9[d]	7LM$^{\gamma Me}$	500/5/1	12	88	168	1.11

[a] Conditions: monomer (M) = 1 mmol, base (B) = ^{t}Bu-P$_4$, activator (A) = *N*-benzoyl-substituted 7LM, at 80 °C, in neat (except for runs 3–6 where a small amount (0.05 mL) of solvent used to liquify monomer at 80 °C). [b] Determined by ^{1}H NMR in DMSO-d_6 or TFA-d_1. [c] Number-average molar mass (M_n) and dispersity index ($Đ = M_w/M_n$) determined via gel permeation chromatography (GPC) coupled with an 18-angle light scattering detector. [d] 5 mmol monomer.

© 2024 The Authors. Angewandte Chemie International Edition published by Wiley-VCH GmbH

15213773, 2024, 17, Downloaded from https://onlinelibrary.wiley.com/doi/10.1002/anie.202320214 by Northwestern University Libraries, Wiley Online Library on [10/07/2024]. See the Terms and Conditions (https://onlinelibrary.wiley.com/terms-and-conditions) on Wiley Online Library for rules of use; OA articles are governed by the applicable Creative Commons License

sion at 80 °C for 12 h, affording nylon $6^{\gamma Me2}$ with M_n = 47.2 kDa, $Đ$ = 1.41 at a [monomer]/[base]/[activator] ([M]/[B]/[A]) ratio of 500/5/1 (Table 1, run 4). This similar condition was then applied to the ROP of $7LM^{\delta Me2}$ and $7LM^{\gamma Me}$, affording nylon $6^{\delta Me2}$ and γ-monomethyl nylon 6 (nylon $6^{\gamma Me}$) with higher monomer conversions, higher polymer molecular weight, and lower dispersity: M_n = 68.1 kDa, $Đ$ = 1.12 for nylon $6^{\delta Me2}$ (Table 1, run 6) and M_n = 168 kDa, $Đ$ = 1.11 for nylon $6^{\gamma Me}$ (Table 1, run 9). Notably, the high reactivity of the superbase ^{t}Bu-P_4 towards the polymerization of 7LM monomers enabled the use of relatively low reaction temperature (80 °C), which suppresses commonly present transamidation side reactions and results in formation of nylons with relatively low $Đ$ values (1.11–1.41).

Given the high ring strain of $7LM^{\alpha Me2}$ (similar to 7LM) and the moderate ring strain of $7LM^{\varepsilon Me2}$ (close to $7LM^{\gamma Me2}$), we reasoned that the *gem*-dimethyl groups at the α and ε positions would inhibit the polymerization due to steric hindrance. To further support this hypothesis, an Interaction Region Indicator (IRI) analysis of six substituted 7LMs was conducted to illustrate the potential impact of the substitution position on the monomer's chemical nature. As depicted in Figure S1, $7LM^{\alpha Me2}$ exhibits steric hindrance between the *gem*-dimethyl group and the carbonyl group. It's also sterically hindered around the nitrogen atom in $7LM^{\varepsilon Me2}$, supporting the steric argument for their resistance towards the ROP under the current conditions. In the case of $7LM^{\beta Me2}$, the non-polymerization observed under various conditions employed in this study may likely be attributed to its low ring strain (its lowest in the series), yielding a T_c that is too low for effective polymerization.

To experimentally investigate the impact of *gem*-disubstitution on the thermodynamics of ROP, thermodynamic studies of the ROP of $7LM^{\gamma Me2}$, $7LM^{\delta Me2}$, and $7LM^{\gamma Me}$ were performed using a [M]/[B]/[A] ratio of 100/1/1 in DMAc. The standard-state thermodynamic parameters, including enthalpy change (ΔH_p°) and entropy change (ΔS_p°) of polymerization along with the T_c values of monomers, were calculated (Tables S7–S9 and Figures S14–S16). The ΔH_p° values of $7LM^{\gamma Me2}$, $7LM^{\delta Me2}$, and $7LM^{\gamma Me}$ were found to be −8.65, −9.89, and −10.73 kJ mol^{-1} and ΔS_p° values were measured to be −30.26, −33.26, and −30.01 J mol^{-1} K^{-1}, respectively. Thus, the introduction of a single methyl group at the γ position of 7LM *drastically* reduces the T_c (766 °C extrapolated to $[M]_{eq}$ = 1.0 M, calculated using the reported ΔH_p° and ΔS_p° values in bulk, omitting solvent effects)[13b] for 7LM to 84 °C (extrapolated to $[M]_{eq}$ = 1.0 M, or 144 °C based on $[M]_{eq} = [M]_0$ = 1.67 M used for the $[M]_{eq}$ measurements) in $7LM^{\gamma Me}$. Installing two *gem*-dimethyl groups at the γ position further lowers the T_c to only 13 °C (extrapolated to $[M]_{eq}$ = 1.0 M, or 136 °C based on $[M]_{eq} = [M]_0$ = 3.0 M used for the $[M]_{eq}$ measurements) for $7LM^{\gamma Me2}$. Moving the *gem*-dimethyl groups to the δ position results in a slightly higher T_c value of 24 °C (extrapolated to $[M]_{eq}$ = 1.0 M, or 137 °C based on $[M]_{eq} = [M]_0$ = 3.0 M used for the $[M]_{eq}$ measurements) for $7LM^{\delta Me2}$. Such low T_c values for $7LM^{\gamma Me2}$ and $7LM^{\delta Me2}$ are consistent with their calculated RSEs and observed moderate polymerizability, suggesting that the depolymerization of their corresponding polymers may be more attainable.

Encouraged by the reduced T_c values in the *gem*-dimethylated 7LMs, we selected nylon $6^{\gamma Me2}$ as a model polymer to probe the CRM effectiveness (Tables 2 and S10) in bulk (solventless) conditions. Nylon $6^{\gamma Me2}$ was subjected to varying temperatures and catalysts under vacuum conditions (10^{-1} Torr). Considering the relatively low T_c of nylon $6^{\gamma Me2}$ (~13 °C in 1.0 M), uncatalyzed thermolysis was initially conducted at a heating mantle temperature of 260 °C for 18 h, giving $7LM^{\gamma Me2}$ in 80 % mass recovery, albeit with (~9 %) impurities (Table 2, run 1). The thermolysis at lower temperatures (e.g., 240 °C) did not produce monomer (Table 2, run 2). Next, various catalysts were screened, aiming to lower the recycling temperature and improve reactivity and/or selectivity. *Ansa*-metallocene $Me_2SiCp''_2YCH(TMS)_2$ ($Cp'' = \eta^5$-Me_4C_5) has been demonstrated as a leading robust catalyst to depolymerize nylon 6 to 7LM with high yields (> 99 %).[12] Thus, this *ansa*-yttrocene catalyst was employed to catalyze the solventless depolymerization of nylon $6^{\gamma Me2}$, effectively yielding 93 % $7LM^{\gamma Me2}$ at 260 °C for 1 h with only 1 mol % catalyst loading (Table 2, run 3). The reaction temperature was further reduced to 240 °C with 90 % yield for pure $7LM^{\gamma Me2}$ in 3 h (Table 2, run 4). We also tested $ZnCl_2$ (10 wt %), a commonly used Lewis acid catalyst for depolymerizing polyesters[21] and nylon,[20g] resulting in a 78 % yield of $7LM^{\gamma Me2}$ at 240 °C after 12 h (Table 2, run 5). Finally, we found that ^{t}BuOK, an inexpensive base, significantly improves reactivity and reduces the recycling temperature (Table S10, runs 7–10). Notably, the depolymerization of nylon $6^{\gamma Me2}$ (M_n = 47.2 kDa, $Đ$ = 1.41) at 180 °C for 6 h with ^{t}BuOK (10 wt %) recovered $7LM^{\gamma Me2}$ in 93 % isolated yield (Table 2, run 6, and Figure 1B). Furthermore, recognizing that nylon recycling often involves mixtures with other plastics, we conducted CRM of nylon $6^{\gamma Me2}$ in the presence of polyethylene (PE), isotactic polypropylene (PP), and polystyrene (PS), selectively affording the nylon monomer $7LM^{\gamma Me2}$ in 87 % yield (Table 2, run 7). The recovered

Table 2: Selected results for depolymerization of nylon $6^{\gamma Me2}$ and nylon $6^{\delta Me2}$.[a]

Run	Polymer	Catalyst	T[b] (°C)	Time (h)	Yield[c] (%)
1	nylon $6^{\gamma Me2}$	none	260	18	80[d]
2	nylon $6^{\gamma Me2}$	none	240	24	0
3[e]	nylon $6^{\gamma Me2}$	[Y] (1 mol %)	260	1	93
4[e]	nylon $6^{\gamma Me2}$	[Y] (1 mol %)	240	3	90
5	nylon $6^{\gamma Me2}$	$ZnCl_2$ (10 wt %)	240	12	78
6[f]	nylon $6^{\gamma Me2}$	^{t}BuOK (10 wt %)	180	6	93[g]
7[h]	nylon $6^{\gamma Me2}$	^{t}BuOK (10 wt %)	180	6	87[g]
8[f]	nylon $6^{\delta Me2}$	^{t}BuOK (10 wt %)	250	18	81[g]

[a] Conditions: polymer (0.10 g, M_n = 20.4, $Đ$ = 1.31 or M_n = 24.0 kDa, $Đ$ = 1.33), under 10^{-1} Torr, [Y] = $Me_2SiCp''_2YCH(TMS)_2$ ($Cp'' = \eta^5$-Me_4C_5). [b] Temperature of the thermocouple-controlled heating mantle. [c] NMR yield using mesitylene as an internal standard. [d] Mass recovery. [e] 10^{-3} Torr. [f] Polymer (0.50 g). [g] Isolated yield. [h] Nylon $6^{\gamma Me2}$ (0.50 g, M_n = 47.2 kDa, $Đ$ = 1.41) with 0.50 g PE, 0.50 g PP, and 0.50 g PS.

© 2024 The Authors. Angewandte Chemie International Edition published by Wiley-VCH GmbH

15213773, 2024, 17, Downloaded from https://onlinelibrary.wiley.com/doi/10.1002/anie.202320214 by Northwestern University Libraries, Wiley Online Library on [10/07/2024]. See the Terms and Conditions (https://onlinelibrary.wiley.com/terms-and-conditions) on Wiley Online Library for rules of use; OA articles are governed by the applicable Creative Commons License

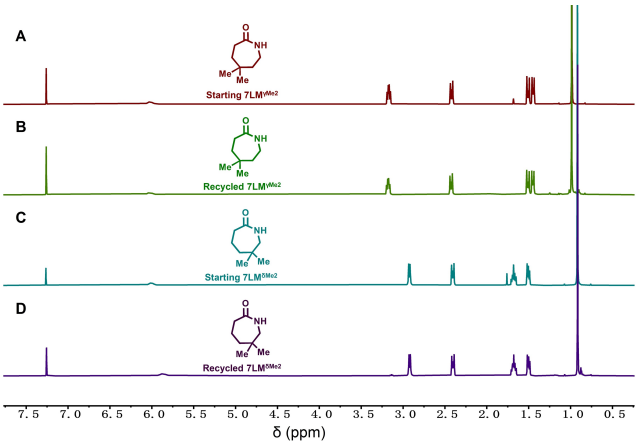

Figure 1. Demonstration of the chemical recycling to monomer. ^{1}H NMR spectra ($CDCl_3$, 25 °C): (**A**) starting 7LM$^{\gamma Me2}$; (**B**) recovered crude 7LM$^{\gamma Me2}$ from catalyzed depolymerization at 180 °C; (**C**) starting 7LM$^{\delta Me2}$; and (**D**) recovered crude 7LM$^{\delta Me2}$ from catalyzed depolymerization at 250 °C.

7LM$^{\gamma Me2}$, after purification, was readily repolymerized into nylon 6$^{\gamma Me2}$ with M_n = 43.5 kDa, $Đ$ = 1.24. Similarly, nylon 6$^{\delta Me2}$ was also subjected to ^{t}BuOK (10 wt %) at 250 °C for 18 h, offering an 81 % isolated yield of 7LM$^{\delta Me2}$ (Table 2, run 8, and Figure 1D).

Thermogravimetric analysis (TGA) of nylon 6$^{\gamma Me2}$ and nylon 6$^{\delta Me2}$ revealed high onset decomposition temperatures at 5 % mass loss ($T_{d,5\%}$) of 360 °C and 351 °C, respectively (Figure 2A), which are 35–44 °C lower than parent nylon 6 ($T_{d,5\%}$ = 395 °C). However, as shown by differential scanning calorimetry (DSC) analysis, the glass transition temperature (T_g) of nylon 6$^{\gamma Me2}$ (91 °C) or nylon 6$^{\delta Me2}$ (93 °C) is considerably higher than the T_g of nylon 6 (50–75 °C),[22] attributable to the *gem*-dimethyl substitution that rigidifies the chain. The *gem*-dimethyl substitution also significantly impacts crystallization behavior and subsequently affects the crystallinity of these nylons. While nylon 6 is a highly crystalline material with a high melting temperature (T_m) of 220 °C (Figure 2B, red), nylon 6$^{\gamma Me2}$ does not crystallize and thus remains amorphous, displaying only a T_g but no T_m peak on DSC scans with a cooling rate of 10 °C/min or 1 °C/min (Figure 2B, black). In contrast, by moving the *gem*-dimethyl substitution to the δ-position of nylon 6, nylon 6$^{\delta Me2}$ exhibits a T_m of 167 °C on the first DSC heating scan (Figure 2B, blue), but not on the second scan, indicating its slow crystallization. Overall, the position of *gem*-dimethyl groups significantly influences the crystallinity of these *gem*-dimethylated nylon 6 materials. Specifically, the *gem*-dimethyl groups at the γ position result in amorphous nylon 6$^{\gamma Me2}$, whereas the δ position produces semi-crystalline nylon 6$^{\delta Me2}$ with slow crystallization. This distinction is confirmed by their powder X-ray diffraction (pXRD) profiles, where the profile of nylon 6$^{\gamma Me2}$ exhibits a broad peak, while nylon 6$^{\delta Me2}$ features sharp diffraction peaks at 2θ values of 9.2°, 18.3°, 23.6° (Figure 2C).

Figure 2D compares the mechanical properties (uniaxial stress-strain curves) of nylon 6, nylon 6$^{\gamma Me2}$, and nylon 6$^{\delta Me2}$. Compression-molded dog-bone-shaped specimens of ny-

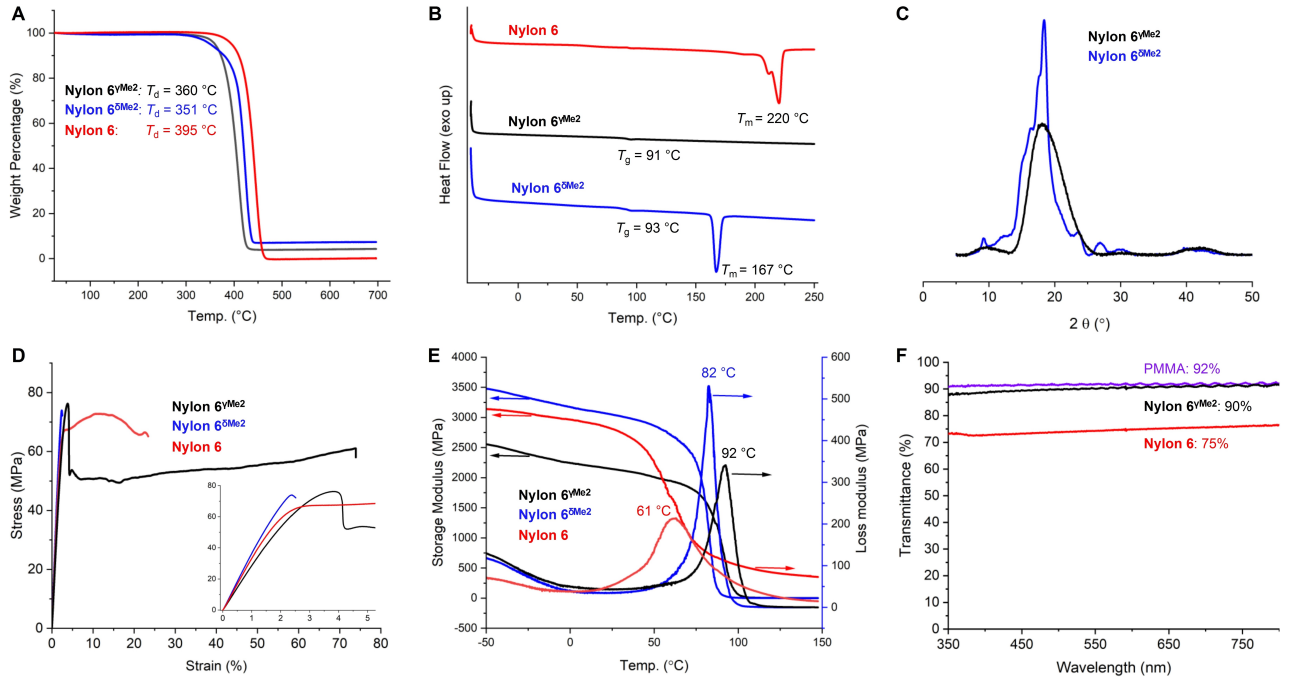

Figure 2. Thermal, mechanical, and optical properties of nylon 6$^{\gamma Me2}$ (black curves) and nylon 6$^{\delta Me2}$ (blue curves), in reference to commercial nylon 6 (red curves): (**A**) TGA thermograms (10 °C/min); (**B**) DSC thermograms of the first heating scan for nylon 6$^{\delta Me2}$ and the second hearting scans for nylon 6 and nylon 6$^{\gamma Me2}$ (10 °C/min); (**C**) pXRD profiles; (**D**) Overlays of representative stress-strain curves; (**E**) DMA (tension film mode) thermomechanical profiles; (**F**) Transmittance overlays of nylon 6$^{\gamma Me2}$, commercial nylon 6, and PMMA (purple line).

© 2024 The Authors. Angewandte Chemie International Edition published by Wiley-VCH GmbH

15213773, 2024, 17, Downloaded from https://onlinelibrary.wiley.com/doi/10.1002/anie.202320214 by Northwestern University Libraries, Wiley Online Library on [10/07/2024]. See the Terms and Conditions (https://onlinelibrary.wiley.com/terms-and-conditions) on Wiley Online Library for rules of use; OA articles are governed by the applicable Creative Commons License

lon $6^{\gamma Me2}$ ($M_n = 47.2$ kDa) exhibit a high elastic modulus (E) of 2.79 ± 0.21 GPa and a high ultimate tensile strength (σ_B) of 60.5 ± 0.60 MPa, which are comparable to those of commercial nylon 6 ($E = 3.37 \pm 0.10$ GPa, $\sigma_B = 65.6 \pm 0.50$ MPa). Remarkably, the amorphous nature of nylon $6^{\gamma Me2}$ does not diminish its mechanical properties; instead, the performance of the polymer is significantly improved, as evidenced by enhanced yield stress ($\sigma_y = 74 \pm 5.4$ MPa) and fracture strain or elongation at break ($\varepsilon_B = 70.2 \pm 7.5\,\%$), compared to crystalline nylon 6 ($\sigma_y = 72.5 \pm 0.8$ MPa, $\varepsilon_B = 25.9 \pm 11.6\,\%$). In comparison, the semi-crystalline nylon $6^{\delta Me2}$ ($M_n = 68.1$ kDa) displays a higher E of 3.55 ± 0.17 GPa and σ_B of 70.7 ± 5.0 MPa, but it is extremely brittle with a small ε_B of only $2.7 \pm 0.2\,\%$.

Dynamic thermomechanical properties of these three nylons were investigated via dynamic mechanical analysis (DMA) in a tension film mode (Figure 2E). Compared to nylon 6 with a storage modulus (E') of 2.81 GPa and a loss modulus (E'') of 53.2 MPa at 25 °C (the glassy state), amorphous nylon $6^{\gamma Me2}$ exhibited lower moduli ($E' = 2.17$ GPa, $E'' = 43.0$ MPa), while semi-crystalline nylon $6^{\delta Me2}$ showed a higher E' of 3.05 GPa and lower E'' of 34.8 MPa. The T_g values, taken from the peak maxima on the loss modulus curve, were 61, 92, and 82 °C for nylon 6, nylon $6^{\gamma Me2}$, and nylon $6^{\delta Me2}$, respectively.

In recent years, optically transparent nylons have found widespread application in automotive, optical instruments, and packaging, due to their high transparency, coupled with the exceptional properties characteristic of nylons.[23,24] Since transparent nylons are typically amorphous,[23] the optical properties of amorphous nylon $6^{\gamma Me2}$ were examined (Figure 2F). Analysis of its transmittance revealed that nylon $6^{\gamma Me2}$ is indeed optically clear. It exhibits a transmittance value (T%) of 90 % when scanned in the visible range (350 to 800 nm). Its transparency is nearly equivalent to that of poly(methyl methacrylate) (PMMA) (T% = 92 %), an optically clear polymer standard, and largely surpasses that of nylon 6 (T% = 75 %), suggesting that nylon $6^{\gamma Me2}$ could serve as a circular nylon for transparent nylon applications.

In summary, in search for alternatives to nylon 6 with enhanced chemical recyclability, mechanical ductility, and optical clarity, we introduced *gem*-dimethyl groups into the ε-caprolactam ring at various positions (α to ε) to investigate redesigned lactam monomer structure/reactivity and the corresponding nylon product structure/property relationships. Four key fundamental insights have been gained from this study. First, the *gem*-dimethyl disubstitution on the seven-membered lactam ring dramatically reduces the T_c of these redesigned 7LM monomers (by >700 °C), making chemical recycling of the resulting *gem*-dimethylated nylon 6 materials to the corresponding monomers more efficient, under milder (60 °C lower temperature) conditions with cheaper, more accessible catalysts. Second, the reactivity or polymerizability of 7LM monomers is highly sensitive to the position of substitution. While *gem*-dimethyl substitutions at the α, β, and ε positions of the 7LM ring yield monomers that exhibit negligible polymerization activity under the conditions employed in this study (due to combined steric and RSE factors), substitutions at γ and δ positions afford 7LM monomers that can be readily polymerized to the corresponding nylons with high molecular weights and low dispersities. Third, the thermomechanical properties of the *gem*-dimethylated nylons also largely depend on the position of disubstitution. While δ-*gem*-dimethylated nylon $6^{\delta Me2}$ is semi-crystalline but more brittle than nylon 6, γ-*gem*-dimethylated nylon $6^{\gamma Me2}$ is an amorphous nylon but with much higher T_g (by 30 °C), yield stress (σ_y by 1.5 MPa), and ductility ($3 \times \varepsilon_B$) than nylon 6. Fourth, redesigned nylon $6^{\gamma Me2}$, with its combined desirable properties of high mechanical performance, closed-loop recyclability, and excellent optical transparency, presents itself as a promising candidate for applications where exceptional properties and optical clarity of polymer are desired. As nylon's optical clarity is often achieved via copolymerization with monomers that can suppress crystallization, which not only increases production costs but also complicates post-consumer nylon recycling by chemical, mechanical, or emerging recycling processes, the single-monomer approach presented herein further highlights the potential of circular polymer design strategies for achieving synergistic outcomes of high chemical recyclability and superior or unique (often surprising, the case here) materials properties.

Acknowledgements

This work was supported by RePLACE (Redesigning Polymers to Leverage A Circular Economy) funded by the Office of Science of the U.S. Department of Energy via award # DE-SC0022290. We thank Clarissa Lincoln of the National Renewable Energy Laboratory for GPC analysis of nylon $6^{\delta Me2}$ samples that require hexafluoro-2-propanol to solubilize them.

Conflict of Interest

The authors declare no conflict of interest.

Data Availability Statement

The data that support the findings of this study are available in the supplementary material of this article.

Keywords: chemical recycling · nylon 6 · monomer design · geminal disubstitution · transparent nylon

[1] a) B. Herzog, M. I. Kohan, S. A. Mestemacher, R. U. Pagilagan, K. Redmond, R. Sarbandi, *Ullmann's Encyclopedia of Industrial Chemistry*, Wiley, Hoboken **2000**, pp. 1–47; b) B. Deopura, R. Alagirusamy, M. Joshi, B. Gupta, *Polyesters and polyamides*, Elsevier, Amsterdam **2008**.

[2] a) *Polyamide-6 Market—Forecast (2022–2027)*, Furion analytics Research & Consulting LLP, Hyderabad **2019**; b) in *Nylon—Global Market Trajectory & Analytics*, Global Industry Analysts, San Jose **2021**; c) *Nylon Market Size, Share & Trends*

© 2024 The Authors. Angewandte Chemie International Edition published by Wiley-VCH GmbH

15213773, 2024, 17, Downloaded from https://onlinelibrary.wiley.com/doi/10.1002/anie.202320214 by Northwestern University Libraries, Wiley Online Library on [10/07/2024]. See the Terms and Conditions (https://onlinelibrary.wiley.com/terms-and-conditions) on Wiley Online Library for rules of use; OA articles are governed by the applicable Creative Commons License

Analysis Report (2023–2030). https://www.grandviewresearch.com/industry-analysis/nylon-6-6-market.
[3] a) Y. Tokiwa, B. P. Calabia, C. U. Ugwu, S. Aiba, *Int. J. Mol. Sci.* **2009**, *10*, 3722–3742; b) K. Min, J. D. Cuiffi, R. T. Mathers, *Nat. Commun.* **2020**, *11*, 727.
[4] a) G. Macfadyen, T. Huntington, R. Cappell, *Regional Seas Reports and Studies* by UNEP, no. 185 **2009**; b) L. Lebreton, B. Slat, F. Ferrari, B. Sainte-Rose, J. Aitken, R. Marthouse, S. Hajbane, S. Cunsolo, A. Schwarz, A. Levivier, K. Noble, P. Debeljak, H. Maral, R. Schoeneich-Argent, R. Brambini, J. Reisser, *Sci. Rep.* **2018**, *8*, 4666.
[5] S. E. Nelms, J. Barnett, A. Brownlow, N. J. Davison, R. Deaville, T. S. Galloway, P. K. Lindeque, D. Santillo, B. J. Godley, *Sci. Rep.* **2019**, *9*, 1075.
[6] a) P. Matthies, W. F. Seydl, *History and Development of Nylon 6*, Springer Netherlands, Dordrecht **1986**, pp. 39–53; b) D. H. Keifer, *The Establishment of Modern Polymer Science by Wallace H. Carothers: An International Historic Chemical Landmark, Wilmington, Delaware, November 17, 2000*, American Chemical Society, Washington **2000**.
[7] G. Hole, A. S. Hole, *Sustain. Prod. Consump.* **2020**, *23*, 42–51.
[8] R. Geyer, J. R. Jambeck, K. L. Law, *Sci. Adv.* **2017**, *3*, e1700782.
[9] a) M. Hong, E. Y.-X. Chen, *Green Chem.* **2017**, *19*, 3692–3706; b) X. Tang, E. Y.-X. Chen, *Chem* **2019**, *5*, 284–312; c) G. W. Coates, Y. D. Y. L. Getzler, *Nat. Rev. Mater.* **2020**, *5*, 501–516; d) V. Hirschberg, D. Rodrigue, *J. Polym. Sci.* **2023**, *61*, 1937–1958; e) A.-J. Minor, R. Goldhahn, L. Rihko-Struckmann, K. Sundmacher, *Chem. Eng. J.* **2023**, *474*, 145333.
[10] a) A. Kamimura, S. Yamamoto, *Polym. Adv. Technol.* **2008**, *19*, 1391–1395; b) S. Yamamoto, A. Kamimura, *Chem. Lett.* **2009**, *38*, 1016–1017; c) A. Kamimura, Y. Shiramatsu, T. Kawamoto, *Green Energy & Environ.* **2019**, *4*, 166–170.
[11] A. Kumar, N. V. Wolff, M. Rauch, Y.-Q. Zou, G. Shmul, Y. Ben-David, G. Leitus, L. Avram, D. Milstein, *J. Am. Chem. Soc.* **2020**, *142*, 14267–14275.
[12] a) L. Wursthorn, K. Beckett, J. O. Rothbaum, R. M. Cywar, C. Lincoln, Y. Kratish, T. J. Marks, *Angew. Chem. Int. Ed.* **2023**, *62*, e202212543; b) L. Ye, X Liu, K. Beckett, J. O. Rothbaum, C. Lincoln, L. J. Broadbelt, Y. Kratish, T. J. Marks, *Chem* **2023**, *10*, 172–189. .
[13] a) A. Duda, A. Kowalski, in *Handbook of Ring-Opening Polymerization*, P. Dubois, O. Coulembier, J.-M. Raquez, eds., Wiley-VCH: Weinheim, Germany **2009**; Ch. 1, pp. 1–52; b) S. Russo, E. Casazza, *Ring-Opening Polymerization of Cyclic Amides (Lactams)*, Elsevier, Amsterdam **2012**, pp. 331–396.
[14] a) C. Shi, L. T. Reilly, V. S. P. Kumar, M. W. Coile, S. R. Nicholson, L. J. Broadbelt, G. T. Beckham, E. Y.-X. Chen, *Chem* **2021**, *7*, 2896–2912; b) C. Shi, L. T. Reilly, E. Y.-X. Chen, *Angew. Chem. Int. Ed.* **2023**, *62*, e202301850.
[15] a) M. E. Jung, G. Piizzi, *Chem. Rev.* **2005**, *105*, 1735–1766; b) S. M. Bachrach, *J. Org. Chem.* **2008**, *73*, 2466–2468.
[16] a) W. Xiong, W. Chang, D. Shi, L. Yang, Z. Tian, H. Wang, Z. Zhang, X. Zhou, E.-Q. Chen, H. Lu, *Chem* **2020**, *6*, 1831–1843; b) Y.-M. Tu, X.-M. Wang, X. Yang, H.-Z. Fan, F.-L. Gong, Z. Cai, J.-B. Zhu, *J. Am. Chem. Soc.* **2021**, *143*, 20591–20597; c) J. Zhou, D. Sathe, J. Wang, *J. Am. Chem. Soc.* **2022**, *144*, 928–934; d) Y.-M. Tu, F.-L. Gong, Y.-C. Wu, Z. Cai, J.-B. Zhu, *Nat. Commun.* **2023**, *14*, 3198.
[17] L. Zhou, Z. Zhang, C. Shi, M. Scoti, D. K. Barange, R. R. Gowda, E. Y.-X. Chen, *Science* **2023**, *380*, 64–69.
[18] X.-L. Li, R. W. Clarke, J.-Y. Jiang, T.-Q. Xu, E. Y.-X. Chen, *Nat. Chem.* **2023**, *15*, 278–285.
[19] a) K. Hashimoto, *Prog. Polym. Sci.* **2000**, *25*, 1411–1462; b) T. Ageyeva, I. Sibikin, J. Karger-Kocsis, *Polymer* **2018**, *10*, 357; c) M. Varghese, M. W. Grinstaff, *Chem. Soc. Rev.* **2022**, *51*, 8258.
[20] a) H. Yang, J. Zhao, M. Yan, S. Pispas, G. Zhang, *Polym. Chem.* **2011**, *2*, 2888; b) Y. Tao, X. Chen, F. Jia, S. Wang, C. Xiao, F. Cui, Y. Li, Z. Bian, X. Chen, X. Wang, *Chem. Sci.* **2015**, *6*, 6385; c) M. Winnacker, M. Neumeier, X. Zhang, C. M. Papadakis, B. Rieger, *Macromol. Rapid Commun.* **2016**, *37*, 851–857; d) P. N. Stockmann, D. L. Pastoetter, M. Woelbing, C. Falcke, M. Winnacker, H. Strittmatter, V. Sieber, *Macromol. Rapid Commun.* **2019**, *40*, 1800903; e) P. N. Stockmann, D. Van Opdenbosch, A. Poethig, D. L. Pastoetter, M. Hoehenberger, S. Lessig, J. Raab, M. Woelbing, C. Falcke, M. Winnacker, C. Zollfrank, H. Strittmatter, V. Sieber, *Nat. Commun.* **2020**, *11*, 509; f) J. Chen, Y. Dong, C. Xiao, Y. Tao, X. Wang, *Macromolecules* **2021**, *54*, 2226–2231; g) J. Lian, J. Chen, S. Luan, W. Liu, B. Zong, Y. Tao, X. Wang, *ACS Macro Lett.* **2022**, *11*, 46–52; h) R. M. Cywar, N. A. Rorrer, H. B. Mayes, A. K. Maurya, C. J. Tassone, G. T. Beckham, E. Y.-X. Chen, *J. Am. Chem. Soc.* **2022**, *144*, 5366–5376.
[21] a) J.-B. Zhu, E. M. Watson, J. Tang, E. Y.-X. Chen, *Science* **2018**, *360*, 398–403; b) X.-L. Li, R. W. Clarke, H.-Y. An, R. R. Gowda, J.-Y. Jiang, T.-Q. Xu, E. Y.-X. Chen, *Angew. Chem. Int. Ed.* **2023**, *62*, e202303791; c) C. F. Gallin, W.-W. Lee, J. A. Byers, *Angew. Chem. Int. Ed.* **2023**, *62*, e202303762; d) J.-B. Zhu, E. M. Watson, J. Tang, E. Y.-X. Chen, *Science* **2018**, *360*, 398–403.
[22] G. Wypych, *Handbook of Polymers, Second Edition*, ChemTec Publishing, Canada **2016**, pp. 215–220.
[23] a) S. Bisoi, A. K. Mandal, A. Singh, V. Padmanabhan, S. Banerjee, *Polym. Chem.* **2017**, *8*, 4220; b) G. Zou, P. Wang, W. Feng, Z. Ren, J. Ji, *J. Appl. Polym. Sci.* **2019**, DOI: 10.1002/APP.47305; c) H. Lao, N. Mushtaq, G. Chen, H. Jiang, Y. Jiao, A. Zhang, X. Fang, *Polymer* **2020**, *206*, 122889; d) C. Zhou, S. Dong, P. Zhu, J. Liu, D. Wang, X. Dong, *Polymer* **2021**, *13*, 1028.
[24] Transparent Polyamide Market Research Report Information. https://www.marketresearchfuture.com/reports/transparent-polyamides-market-8032.

Manuscript received: December 29, 2023
Accepted manuscript online: February 28, 2024
Version of record online: March 15, 2024

© 2024 The Authors. Angewandte Chemie International Edition published by Wiley-VCH GmbH

15213773, 2024, 17, Downloaded from https://onlinelibrary.wiley.com/doi/10.1002/anie.202320214 by Northwestern University Libraries, Wiley Online Library on [10/07/2024]. See the Terms and Conditions (https://onlinelibrary.wiley.com/terms-and-conditions) on Wiley Online Library for rules of use; OA articles are governed by the applicable Creative Commons License